The following resources related to this article are available online at
www.sciencemag.org (this information is current as of May 17, 2007):

Updated information and services, including high-resolution figures, can be found in the online version of this article at:
http://www.sciencemag.org/cgi/content/full/316/5826/889

Supporting Online Material can be found at:
http://www.sciencemag.org/cgi/content/full/1141634/DC1

A list of selected additional articles on the Science Web sites **related to this article** can be found at:
http://www.sciencemag.org/cgi/content/full/316/5826/889#related-content

This article **cites 18 articles**, 7 of which can be accessed for free:
http://www.sciencemag.org/cgi/content/full/316/5826/889#otherarticles

This article appears in the following **subject collections**:
Genetics
http://www.sciencemag.org/cgi/collection/genetics

Information about obtaining **reprints** of this article or about obtaining **permission to reproduce this article** in whole or in part can be found at:
http://www.sciencemag.org/about/permissions.dtl

at bead surfaces or sites of TCR ligation then displaces the bound IP_4 (fig. S6A). The ability of soluble PIP_3 to modulate Itk binding to PIP_3-coated beads with a dose response similar to that of IP_4 (fig. S5, C and D) is consistent with this "induced-fit model." An attractive alternative model is suggested by our finding that the Itk PH domain aggregates with other Itk PH domain fragments or full-length Itk in a manner unaffected by 10 μM IP_4 (Fig. 4F). IP_4 binding to one PH domain might induce conformational changes in the other subunits that increase their affinities for PIP_3 allosterically (fig. S6B). Future research will distinguish between these models and conclusively determine the precise mechanism by which IP_4 augments PH domain interactions with PIP_3.

Our results show that IP_4 acts as an essential mediator of Itk and PLC-γ1 activation and DAG production in DP thymocytes through Itk recruitment to sites of TCR engagement (fig. S7). This IP_4 function is essential for TCR signaling during thymocyte positive selection. Besides Itk, low-micromolar concentrations of IP_4 also augmented PIP_3 interactions of several other PH domain proteins, including Tec and GAP1^{IP4BP} (3, 13–15) (Fig. 4, A and B). In particular, IP_4 augmented PIP_3 binding of GAP1^{IP4BP} PH domain fragments (fig. S5E). Dysregulation of several IP_4-regulated PH domain proteins could explain the phenotypic differences between ItpkB$^{-/-}$ (2, 3) and Itk$^{-/-}$ mice (6). By contrast, PH domain–dependent PLC-γ1 binding to PIP_3-coated beads was unaffected by IP_4 (Fig. 4, A and B). Thus, positive or negative regulation of PIP_3 binding through soluble IP_4 may serve as a general mechanism that controls membrane recruitment of a group of PIP_3-binding proteins in a specific manner (Fig. 4 and fig. S5) (16). It will be interesting to determine whether defects in this mechanism of IP_4 action contribute to the impaired B cell development and function in ItpkB$^{-/-}$ mice, as reported in (17). PIP_3-binding proteins and IP_4 exist in all eukaryotes. Thus, IP_4 modulation of PH domain function likely has global implications.

References and Notes

1. T. K. Starr, S. C. Jameson, K. A. Hogquist, *Annu. Rev. Immunol.* **21**, 139 (2003).
2. V. Pouillon *et al.*, *Nat. Immunol.* **4**, 1136 (2003).
3. B. G. Wen *et al.*, *Proc. Natl. Acad. Sci. U.S.A.* **101**, 5604 (2004).
4. J. P. Roose, M. Mollenauer, V. A. Gupta, J. Stone, A. Weiss, *Mol. Cell. Biol.* **25**, 4426 (2005).
5. See supporting material on *Science* Online.
6. L. J. Berg, L. D. Finkelstein, J. A. Lucas, P. L. Schwartzberg, *Annu. Rev. Immunol.* **23**, 549 (2005).
7. M. Fukuda, T. Kojima, H. Kabayama, K. Mikoshiba, *J. Biol. Chem.* **271**, 30303 (1996).
8. T. Kojima, M. Fukuda, Y. Watanabe, F. Hamazato, K. Mikoshiba, *Biochem. Biophys. Res. Commun.* **236**, 333 (1997).
9. A. August, A. Sadra, B. Dupont, H. Hanafusa, *Proc. Natl. Acad. Sci. U.S.A.* **94**, 11227 (1997).
10. P. S. Costello, M. Gallagher, D. A. Cantrell, *Nat. Immunol.* **3**, 1082 (2002).
11. K. A. Ching, Y. Kawakami, T. Kawakami, C. D. Tsoukas, *J. Immunol.* **163**, 6006 (1999).
12. A. H. Guse, E. Greiner, F. Emmrich, K. Brand, *J. Biol. Chem.* **268**, 7129 (1993).
13. P. J. Cullen *et al.*, *Nature* **376**, 527 (1995).
14. M. Fukuda, K. Mikoshiba, *J. Biol. Chem.* **271**, 18838 (1996).
15. S. Yarwood, D. Bouyoucef-Cherchalli, P. J. Cullen, S. Kupzig, *Biochem. Soc. Trans.* **34**, 846 (2006).
16. R. Stricker, S. Adelt, G. Vogel, G. Reiser, *Eur. J. Biochem.* **265**, 815 (1999).
17. A. T. Miller *et al.*, *Nat. Immunol.* **8**, 514 (2007).
18. C. J. Serrano *et al.*, *J. Immunol.* **174**, 6233 (2005).
19. We thank J. Alberola-Ila, A. Altman, N. Gascoigne, T. Kawakami, G. Koretzky, L. Min, K. Mowen, R. Reisfeld, and C. Schmedt for discussions or reading of the manuscript; R. Kay for mice; and C. Dubord-Jackson, M. Young, and the GNF vivarium for mouse handling. Supported by GNF and NIH

A Common Variant in the *FTO* Gene Is Associated with Body Mass Index and Predisposes to Childhood and Adult Obesity

Timothy M. Frayling,[1,2]* Nicholas J. Timpson,[3,4]* Michael N. Weedon,[1,2]* Eleftheria Zeggini,[3,5]* Rachel M. Freathy,[1,2] Cecilia M. Lindgren,[3,5] John R. B. Perry,[1,2] Katherine S. Elliott,[3] Hana Lango,[1,2] Nigel W. Rayner,[3,5] Beverley Shields,[2] Lorna W. Harries,[2] Jeffrey C. Barrett,[3] Sian Ellard,[2,6] Christopher J. Groves,[5] Bridget Knight,[2] Ann-Marie Patch,[2,6] Andrew R. Ness,[7] Shah Ebrahim,[8] Debbie A. Lawlor,[9] Susan M. Ring,[9] Yoav Ben-Shlomo,[9] Marjo-Riitta Jarvelin,[10,11] Ulla Sovio,[10,11] Amanda J. Bennett,[5] David Melzer,[1,12] Luigi Ferrucci,[13] Ruth J. F. Loos,[14] Inês Barroso,[15] Nicholas J. Wareham,[14] Fredrik Karpe,[5] Katharine R. Owen,[5] Lon R. Cardon,[3] Mark Walker,[16] Graham A. Hitman,[17] Colin N. A. Palmer,[18] Alex S. F. Doney,[19] Andrew D. Morris,[19] George Davey Smith,[4] The Wellcome Trust Case Control Consortium,† Andrew T. Hattersley,[1,2]‡§ Mark I. McCarthy[3,5]‡

Obesity is a serious international health problem that increases the risk of several common diseases. The genetic factors predisposing to obesity are poorly understood. A genome-wide search for type 2 diabetes–susceptibility genes identified a common variant in the *FTO* (fat mass and obesity associated) gene that predisposes to diabetes through an effect on body mass index (BMI). An additive association of the variant with BMI was replicated in 13 cohorts with 38,759 participants. The 16% of adults who are homozygous for the risk allele weighed about 3 kilograms more and had 1.67-fold increased odds of obesity when compared with those not inheriting a risk allele. This association was observed from age 7 years upward and reflects a specific increase in fat mass.

Obesity is a major cause of morbidity and mortality, associated with an increased risk of type 2 diabetes mellitus, heart disease, metabolic syndrome, hypertension, stroke, and certain forms of cancer. It is typically measured clinically with the surrogate measure of body mass index (BMI), calculated as weight divided by height squared. Individuals with a BMI ≥ 25 kg/m^2 are classified as overweight, and those with a BMI ≥ 30 kg/m^2 are considered obese. The prevalence of obesity is increasing worldwide, probably as the result of changed lifestyle. In 2003–2004, 66% of the U.S. population had a BMI ≥ 25 kg/m^2, and 32% were obese (1).

Twin and adoption studies have demonstrated that genetic factors play an important role in influencing which individuals within a population are most likely to develop obesity in response to a particular environment (2). However,

despite considerable efforts, there are, as yet, no examples of common genetic variants for which there is widely replicated evidence of association with obesity in the general population. Monogenic forms of obesity at present account for ~7% of children with severe, young-onset obesity (3), but as this severity of obesity is only seen in <0.01% of the population, these mutations are rare in the general population. Recent attempts to identify gene variants predisposing to common, polygenic obesity have proven controversial. Initial reports of promising associations between common variants in the *GAD*2 (4–7), *ENPP1* (5, 8, 9) and *INSIG2* (9–12) genes and altered BMI have not been widely replicated.

Obesity is a major risk factor for type 2 diabetes, and variants that influence the development of obesity may also predispose to type 2 diabetes. As part of the Wellcome Trust Case Control

Control Consortium (WTCCC), we recently completed a genome-wide association study comparing 1924 U.K. type 2 diabetes patients and 2938 U.K. population controls for 490,032 autosomal single-nucleotide polymorphisms (SNPs) (Wellcome Trust Case Control Consortium). SNPs in the *FTO* (fat mass and obesity associated) gene region on chromosome 16 were strongly associated with type 2 diabetes (e.g., rs9939609, OR = 1.27; 95% CI = 1.16 to 1.37; $P = 5 \times 10^{-8}$). This association was replicated by analyzing SNP rs9939609 in a further 3757 type 2 diabetes cases and 5346 controls (OR = 1.15; 95% CI = 1.09 to 1.23; $P = 9 \times 10^{-6}$). Analysis of BMI as a continuous trait was possible in the initial diabetes cases and in all replication samples but not in the initial control samples. The diabetes-risk alleles at *FTO* were strongly associated with increased BMI (Table 1). In the replication samples, the association between *FTO* SNPs and type 2 diabetes was abolished by adjustment for BMI (OR = 1.03; 95% CI = 0.96 to 1.10; $P = 0.44$), which suggests that the association of these SNPs with T2D risk is mediated through BMI. The major signal for association with BMI coincides perfectly with that for type 2 diabetes, and rs9939609 represents a cluster of 10 SNPs in

the first intron of *FTO* that are associated with both traits (Fig. 1). All BMI-associated SNPs (*P* ranging from 1×10^{-4} to 1×10^{-5}) are highly correlated with each other (r^2 from 0.52 to 1.0). SNP rs9939609 was used in all further studies, because among the cluster of most highly associated SNPs it had the highest genotyping success rate (100%). The HapMap (haplotype map of the human genome) population frequencies of the rs9939609 A allele are 0.45 in the CEPH (Centre d'Etude du Polymorphisme Humain) Europeans, 0.52 in Yorubans, and 0.14 in Chinese and Japanese.
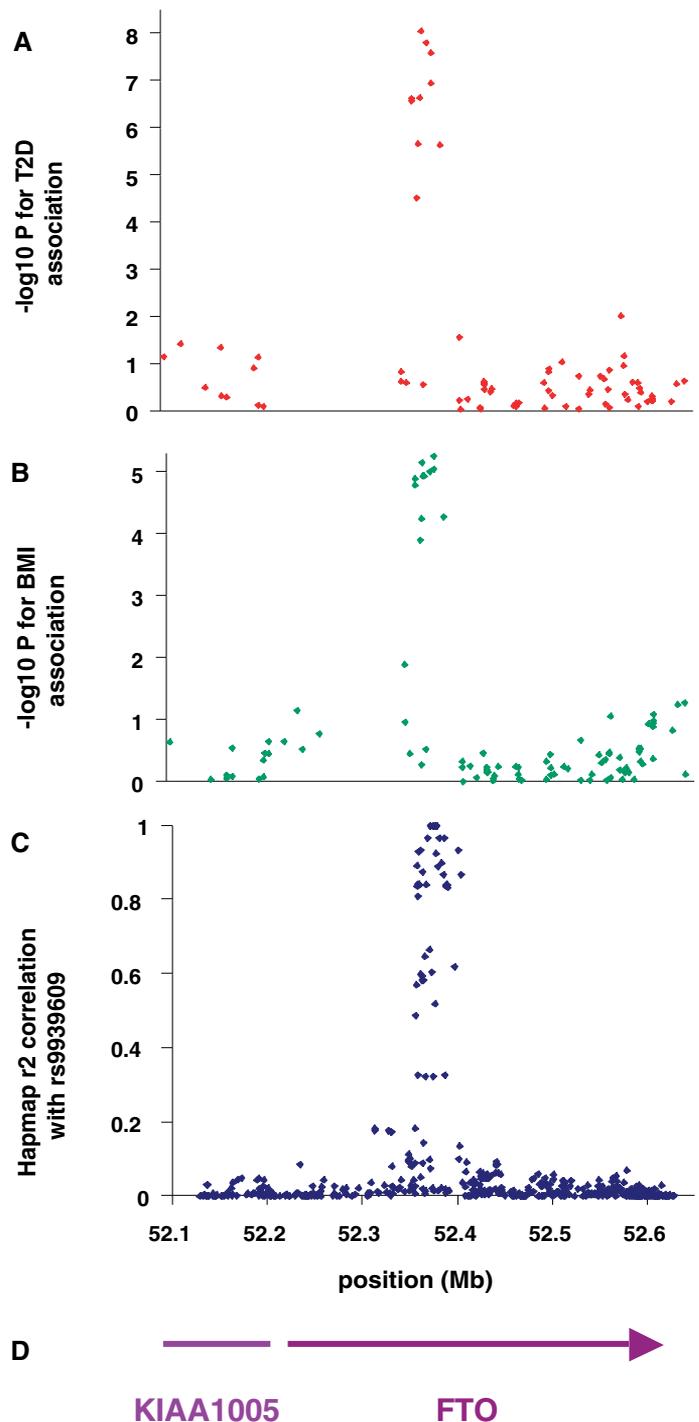
We studied the association of *FTO* gene variation with BMI and the risk of being overweight and obese in an additional 19,424 white European adults from seven general population-based studies (mean age 28 to 74 years, mean BMI 22.7 to 27.2 kg/m^2) and in 10,172 white European children from two studies (mean age 7 to 14 years, mean BMI 16.1 to 19.2 kg/m^2) [table S1 and supporting online text (*13*)].

In all adult population-based studies, we found that the type 2 diabetes–associated A allele of rs9939609 (frequency 39%) was associated with increased BMI (Table 1) with a median per-allele

Fig. 1. Associations of SNPs in the *FTO/KIA1005* region of chromosome 16 with (**A**) type 2 diabetes using 1924 cases and 2938 controls and (**B**) adult BMI in type 2 diabetic patients. (**C**) Linkage disequilibrium (r^2) between associated SNP rs9939609 and all other SNPs in HapMap data in Caucasian European samples. (**D**) Gene positions.

[1]Genetics of Complex Traits, Institute of Biomedical and Clinical Science, Peninsula Medical School, Magdalen Road, Exeter, UK. [2]Diabetes Genetics, Institute of Biomedical and Clinical Science, Peninsula Medical School, Barrack Road, Exeter, UK. [3]Wellcome Trust Centre for Human Genetics, University of Oxford, Roosevelt Drive, Oxford, UK. [4]MRC Centre for Causal Analyses in Translational Epidemiology, Bristol University, Canynge Hall, Whiteladies Road, Bristol, UK. [5]Oxford Centre for Diabetes, Endocrinology and Metabolism, University of Oxford, Churchill Hospital, Oxford, UK. [6]Molecular Genetics Laboratory, Royal Devon and Exeter National Health Service Foundation Trust, Old Pathology Building, Barrack Road, Exeter, UK. [7]Department of Oral and Dental Science, University of Bristol Dental School, Lower Maudlin Street, Bristol, UK. [8]Department of Epidemiology and Population Health, London School of Hygiene and Tropical Medicine, London, UK. [9]Department of Social Medicine, University of Bristol, Canynge Hall, Whiteladies Road, Bristol, UK. [10]Department of Epidemiology and Public Health, Imperial College London, Norfolk Place, London W2 1PG, UK. [11]Department of Public Health Science and General Practice, Fin-90014, University of Oulu, Finland. [12]Epidemiology and Public Health Group, Peninsula Medical School, Barrack Road, Exeter, UK. [13]Longitudinal Studies Section, Clinical Research Branch, National Institute on Aging, National Institutes of Health, Baltimore, MD, USA. [14]Medical Research Council Epidemiology Unit, Strangeways Research Laboratories, Cambridge, UK. [15]Metabolic Disease Group, Wellcome Trust Sanger Institute, Hinxton, Cambridge, UK. [16]Diabetes Research Group, School of Clinical Medical Sciences, Newcastle University, Framlington Place, Newcastle upon Tyne, UK. [17]Centre for Diabetes and Metabolic Medicine, Barts and The London, Royal London Hospital, Whitechapel, London, UK. [18]Population Pharmacogenetics Group, Biomedical Research Centre, Ninewells Hospital and Medical School, University of Dundee, Dundee, UK. [19]Diabetes Research Group, Division of Medicine and Therapeutics, Ninewells Hospital and Medical School, University of Dundee, Dundee, UK.

*These authors contributed equally to this work.
†Membership of the Wellcome Trust Case Control Consortium is listed in the Supporting Online Material.
‡These authors contributed equally to this work.
§To whom correspondence should be addressed. E-mail: Andrew.Hattersley@pms.ac.uk

change of ~0.36 kg/m^2 (range 0.34 to 0.46 kg/m^2). In each study, carriers of two A alleles had a higher BMI than heterozygote individuals; when we compared the additive model to a general model in each study, there was no consistent evidence for departure from an additive model. Because there was no evidence of heterogeneity ($I^2 = 0\%$) across the adult studies (*14*), we combined them using the inverse variance method to pool continuous data (Z scores) and the Mantel-Haenszel method for binary data. Each additional copy of the rs9939609 A allele was associated with a BMI increase of a mean of 0.10 Z-score units (95% CI = 0.08 to 0.12; $P = 2 \times 10^{-20}$), equivalent to ~0.4 kg/m^2. When these data were combined with those from the case-control samples (a total of 30,081 participants), the statistical confidence of the association was further increased ($P = 3 \times 10^{-35}$) (Table 1 and fig. S1). When we applied a Bonferroni correction for the number of tests performed in the initial genome-wide scan (~400,000), the association remained significant ($P = 1.2 \times 10^{-29}$). This association was present in adults of all ages (Table 1) and of both sexes (fig. S1B and S1C), with no difference between males and females ($P = 0.13$).

Although BMI is a continuous trait, standard cut-offs are used to assess the burden of increased body weight on health. Hence, we assessed whether the inheritance of the *FTO* SNP rs9939609 altered the risk of being either overweight or obese compared with being normal weight (<25 kg/m^2). In all the studies, the A allele was associated with increased odds of being overweight (Fig. 2A) and also of being obese (Fig. 2B and table S2). In a meta-analysis of the population-based studies, the per-A allele odds ratio (OR) for obesity in the adult general population was 1.31 (95% CI = 1.23 to 1.39; $P = 6 \times 10^{-16}$); for overweight, it was 1.18 (95% CI = 1.13 to 1.24; $P = 1 \times 10^{-12}$). When participants from the type 2 diabetes case and

Table 1. Association of BMI with rs9939609 genotypes, corrected for sex, in type 2 diabetes cases from genome-wide and replication studies, control participants from replication studies, and adult population-based studies. P values represent the change per A allele. BMI presented as geometric means and back-transformed 95% confidence intervals.
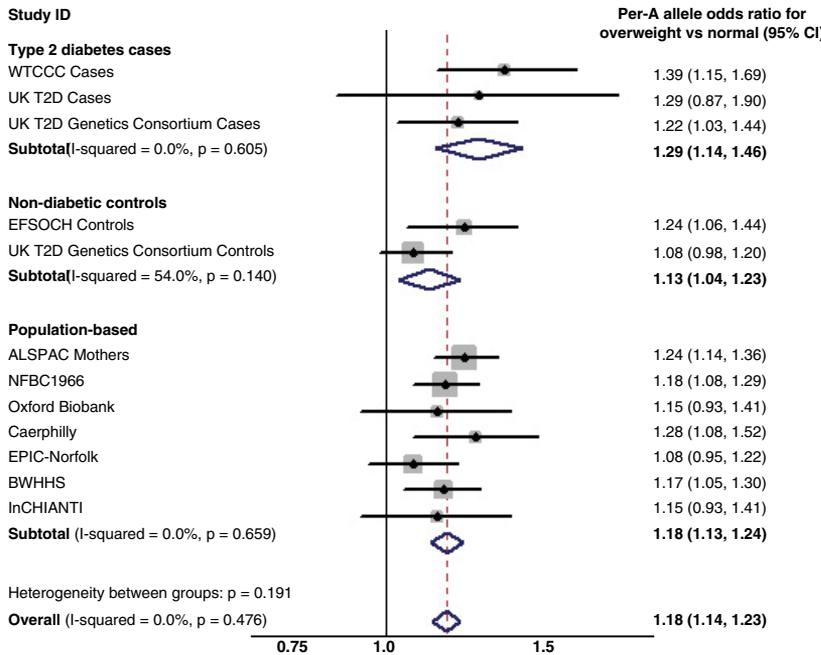
Study	Age, years (mean, SD)	Males (%)	N	Mean BMI (95% CI) by genotype			P
				TT	AT	AA	
Type 2 diabetes							
UK cases (WTCCC)	58.6 (10.3)	58	1913	30.15 (29.69, 30.62)	30.47 (30.12, 30.83)	31.99 (31.39, 32.59)	8×10^{-6}
UK T2D Cases	59.2 (8.6)	58	609	30.89 (30.12, 31.69)	31.14 (30.51, 31.78)	33.46 (32.38, 34.58)	0.001
UKT2D GCC Cases	64.1 (9.6)	57	2961	30.59 (30.24, 30.95)	30.96 (30.67, 31.26)	31.98 (31.48, 32.50)	3×10^{-5}
Combined T2D (I^2)							3×10^{-11} (15.6%)
Nondiabetic controls							
EFSOCH	31.8 (5.6)	51	1746	24.50 (24.21, 24.80)	25.21 (24.95, 25.47)	25.41 (24.92, 25.91)	0.0002
UKT2D GCC Controls	58.8 (11.9)	52	3428	26.25 (26.02, 26.48)	26.34 (26.13, 26.54)	27.07 (26.71, 27.44)	0.001
Population-based studies							
Adult							
ALSPAC (mothers)	28.4 (4.7)	0	6376	22.42 (22.28, 22.56)	22.73 (22.61, 22.85)	23.27 (23.03, 23.51)	3×10^{-10}
NFBC1966 (age 31)	31	48	4435	24.12 (23.94, 24.31)	24.43 (24.26, 24.60)	24.82 (24.53, 25.12)	5×10^{-5}
Oxford Biobank	40.6 (6.1)	55	765	25.48 (25.02, 25.94)	25.36 (24.95, 25.78)	26.43 (25.70, 27.17)	0.09
Older adult							
Caerphilly	56.7 (4.5)	100	1328	26.10 (25.80, 26.40)	26.48 (26.20, 26.76)	26.69 (26.11, 27.28)	0.03
EPIC-Norfolk	59.7 (9.0)	47	2425	25.87 (25.63, 26.11)	26.20 (25.99, 26.42)	26.61 (26.22, 27.01)	0.001
BWHHS	68.8 (5.5)	0	3244	26.77 (26.51, 27.02)	27.33 (27.09, 27.56)	27.58 (27.17, 28.00)	0.0002
InCHIANTI	74.3 (6.9)	45	851	26.99 (26.53, 27.47)	26.99 (26.61, 27.37)	27.84 (27.23, 28.46)	0.06
Combined population studies (I^2)							2×10^{-20} (0%)
Combined population and control studies (I^2)							1×10^{-25} (0%)
All studies (I^2)							3×10^{-35} (0%)

Table 2. Association of BMI (corrected for sex) and birth weight (corrected for sex and gestational age) with rs9939609 genotypes in children. P values represent the change in log BMI per A allele. BMI presented as geometric means and back-transformed 95% confidence intervals.
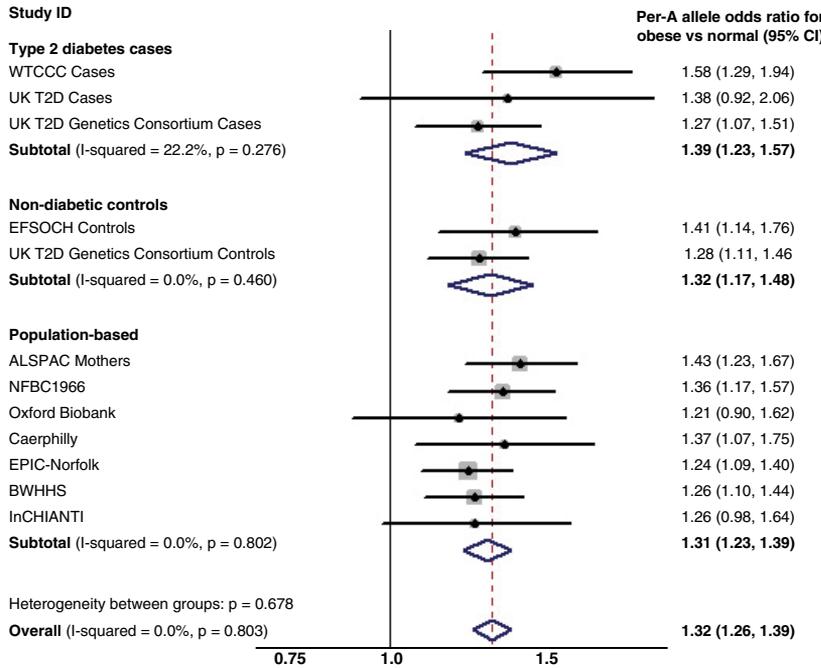
Cohort	Age (years)	Males (%)	N	Mean trait value (95% CI) by genotype			P
				TT	AT	AA	
*Children**							
ALSPAC	7	51	5969	16.00 (15.92, 16.07)	16.11 (16.04, 16.18)	16.31 (16.19, 16.43)	3×10^{-5}
	8	50	4871	16.80 (16.70, 16.90)	17.01 (16.92, 17.09)	17.29 (17.14, 17.45)	1×10^{-7}
	9	50	5459	17.20 (17.08, 17.31)	17.53 (17.43, 17.63)	17.86 (17.69, 18.04)	5×10^{-11}
	10	50	5273	17.66 (17.54, 17.79)	18.05 (17.94, 18.17)	18.37 (18.18, 18.57)	1×10^{-10}
	11	49	5010	18.46 (18.32, 18.61)	18.82 (18.70, 18.94)	19.20 (18.98, 19.42)	7×10^{-9}
NFBC1966 (age 14)	14	47	4203	19.14 (19.02, 19.26)	19.25 (19.14, 19.36)	19.38 (19.19, 19.57)	0.04
Birth†							
ALSPAC	0	51	7477	3438 (3422, 3455)	3452 (3437, 3466)	3454 (3429, 3480)	0.21
NFBC1966	0	47	4320	3523 (3501, 3546)	3538 (3518, 3558)	3536 (3501, 3571)	0.42

*ALSPAC children are offspring of the participants included in the adult study (Table 1), and data are shown at five available ages. NFBC1966 children are the same participants as those in the adult study (Table 1).   †ALSPAC birth data are for the same participants as those in the children study. NFBC1966 birth data are for the same participants as those in the children and adult studies. Non-singleton births and individuals born at gestation <36 weeks were excluded from the birth-weight analysis.
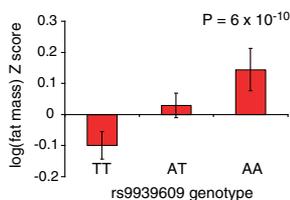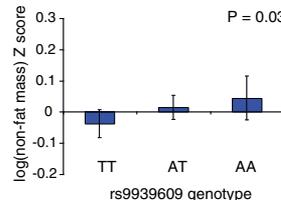
A

Study ID

Per-A allele odds ratio for overweight vs normal (95% CI)

Type 2 diabetes cases
WTCCC Cases 1.39 (1.15, 1.69)
UK T2D Cases 1.29 (0.87, 1.90)
UK T2D Genetics Consortium Cases 1.22 (1.03, 1.44)
Subtotal(I-squared = 0.0%, p = 0.605) .... **1.29 (1.14, 1.46)**

Non-diabetic controls
EFSOCH Controls 1.24 (1.06, 1.44)
UK T2D Genetics Consortium Controls 1.08 (0.98, 1.20)
Subtotal(I-squared = 54.0%, p = 0.140) .... **1.13 (1.04, 1.23)**

Population-based
ALSPAC Mothers 1.24 (1.14, 1.36)
NFBC1966 .... 1.18 (1.08, 1.29)
Oxford Biobank 1.15 (0.93, 1.41)
Caerphilly 1.28 (1.08, 1.52)
EPIC-Norfolk 1.08 (0.95, 1.22)
BWHHS 1.17 (1.05, 1.30)
InCHIANTI 1.15 (0.93, 1.41)
Subtotal (I-squared = 0.0%, p = 0.659) .... **1.18 (1.13, 1.24)**

Heterogeneity between groups: p = 0.191
Overall (I-squared = 0.0%, p = 0.476) .... **1.18 (1.14, 1.23)**

0.75   1.0   1.5

B

Study ID

Per-A allele odds ratio for obese vs normal (95% CI)

Type 2 diabetes cases
WTCCC Cases 1.58 (1.29, 1.94)
UK T2D Cases 1.38 (0.92, 2.06)
UK T2D Genetics Consortium Cases 1.27 (1.07, 1.51)
Subtotal (I-squared = 22.2%, p = 0.276) .... **1.39 (1.23, 1.57)**

Non-diabetic controls
EFSOCH Controls 1.41 (1.14, 1.76)
UK T2D Genetics Consortium Controls 1.28 (1.11, 1.46)
Subtotal (I-squared = 0.0%, p = 0.460) .... **1.32 (1.17, 1.48)**

Population-based
ALSPAC Mothers 1.43 (1.23, 1.67)
NFBC1966 .... 1.36 (1.17, 1.57)
Oxford Biobank 1.21 (0.90, 1.62)
Caerphilly 1.37 (1.07, 1.75)
EPIC-Norfolk 1.24 (1.09, 1.40)
BWHHS 1.26 (1.10, 1.44)
InCHIANTI 1.26 (0.98, 1.64)
Subtotal (I-squared = 0.0%, p = 0.802) .... **1.31 (1.23, 1.39)**

Heterogeneity between groups: p = 0.678
Overall (I-squared = 0.0%, p = 0.803) .... **1.32 (1.26, 1.39)**

0.75   1.0   1.5

C

$P = 6 \times 10^{-10}$

log(fat mass) Z score — rs9939609 genotype: TT, AT, AA

D

$P = 0.03$

log(non-fat mass) Z score — rs9939609 genotype: TT, AT, AA

Fig. 2. (**A** and **B**) Meta-analysis plots for odds of (A) overweight and (B) obesity, compared with normal weight in adults for each copy of the A allele of rs9939609 carried. (**C** and **D**) Bar charts showing (C) DEXA-measured fat mass in 9-year-old children and (D) DEXA-measured lean mass in 9-year-old children, both from the ALSPAC study. Error bars represent 95% confidence intervals

control studies were included, the magnitude of the association was unchanged, although the statistical confidence increased (obesity: OR = 1.32; 95% CI 1.26 to 1.39; $P = 3 \times 10^{-26}$; overweight: OR = 1.18; 95% CI 1.14 to 1.23], $P = 2 \times 10^{-17}$). Individuals homozygous for the A allele at rs9939609 (16% of the population) are at substantially increased risk of being overweight (OR = 1.38; 95% CI 1.26 to 1.52]; $P = 4 \times 10^{-11}$) or obese (OR = 1.67; 95% CI = 1.47 to 1.89; $P = 1 \times 10^{-14}$) compared with those homozygous for the low-risk T allele (37% of the population). The extent of the variance in BMI explained by rs9939609 was ~1%, and the population attributable risk was 20.4% for obesity and 12.7% for overweight.

Childhood obesity is also increasing rapidly worldwide and is a cause of considerable concern (15). To determine the age at which the association of *FTO* SNP rs9939609 with BMI first becomes evident, we analyzed two large birth cohorts for which suitable measures were available from birth to early adolescence. These included 7477 UK children from the Avon Longitudinal Study of Parents and Children (ALSPAC) cohort who had anthropometric measures at birth and at 7, 8, 9, 10, and 11 years of age and 4320 children from the Northern Finland 1966 birth cohort (NFBC1966) with birth measures as well as height and weight available at 14 years. rs9939609 was not associated with birth weight (Table 2) or ponderal index at birth (table S3A) in either cohort. In children from the ALSPAC study, each copy of the rs9939609 A allele was associated with an increase in BMI by 0.08 Z-score units (95% CI = 0.04 to 0.12; $P = 3 \times 10^{-5}$; ~0.2 kg/m²) at age 7, an association maintained up to the most recent assessment at age 11, when the per-allele increase was 0.12 Z-score units (95% CI = 0.08 to 0.16; $P = 7 \times 10^{-9}$; ~0.4 kg/m²) (Table 2). At all ages, the A allele was associated with an increased risk of childhood obesity (e.g., OR per-A allele at age 11 years = 1.35; CI = 1.14, 1.61; $P = 6 \times 10^{-4}$) and of being overweight (e.g., OR per-A allele at age 11 years = 1.27; CI = 1.16 to 1.39; $P = 2 \times 10^{-7}$), as defined by age-specific BMI (table S2). In the Finnish cohort, each copy of the rs9939609 A allele was associated with an increase in BMI by 0.05 Z-score units (95% CI = 0.003 to 0.09; $P = 0.04$; ~0.1 kg/m²) at the age of 14 years (Table 2). We conclude therefore that *FTO* SNP rs9939609 is not associated with changes in fetal growth but is associated with changes in BMI and obesity in children by the age of 7, changes that persist into the prepubertal period and beyond.

BMI is a convenient surrogate measure for obesity, but it may be influenced by changes in height, bone mass, and lean mass, as well as adiposity. We used additional anthropometric measurements available in the study samples to address this issue. In all population-based cohorts, the rs9939609 A allele was associated with higher weight (overall per-A allele increase =

0.09 Z-score units; 95% CI = 0.07 to 0.11); P = 4×10^{-17}; ~1.2 kg in adults) (tables S3B and S3C), but there was no difference in height (tables S3C and S3D). Consistent with this observation, we found evidence for higher waist circumference (overall per-A allele = 0.08 Z-score units; 95% CI = 0.05 to 0.11; P = 4×10^{-9}; ~1 cm) (table S3E) and higher subcutaneous mass assessed by skinfold measures (per-A allele difference = 0.11 Z-score units; 95% CI = 0.06 to 0.16; P = 2×10^{-5}) (table S3F). In the children from the ALSPAC study, dual-energy x-ray absorptiometry (DEXA)–derived measures of fat mass and lean mass were available at age 9. The association of rs9939609 A allele with weight was almost exclusively attributable to changes in fat mass, with a per-allele difference of 0.12 Z-score units (95% CI = 0.08 to 0.16; P = 6×10^{-10}), equivalent to a 14% difference across the three genotype groups) (Fig. 2C). Genotype-related differences in lean mass were, in contrast, a modest 0.04 Z-score units (95% CI = 0.005 to 0.08; P = 0.03), which is equivalent to a 1% increase across the three genotype groups) (Fig. 2D). Therefore, the association of genetic variation at *FTO* with BMI results from longitudinal changes in fat mass that, on the basis of anthropometric measures, reflect both increased waist circumference and subcutaneous fat.

One important potential source of false-positive associations in genetic studies is population stratification. We do not believe this is likely to be important in the association of the *FTO* SNP with BMI or type 2 diabetes. In all study cohorts, any individuals who were not European whites were excluded. In addition the cohorts were all recruited from single countries, with the majority coming from specific small geographically defined regions, and the analysis for association was done only within individual cohorts. Analysis of the *FTO* signal does not support this association resulting from population stratification. In the original genome-wide association study, the principal component analysis (*16*) implemented in EIGENSTRAT (*17*) made no difference to the evidence for association for type 2 diabetes (P = 5.3×10^{-8} with EIGENSTRAT adjustment and 5.2×10^{-8} without). Similarly, adjusting for the 11 geographic regions did not alter the significance of the *FTO* association for BMI (P = 9×10^{-6} adjusted; 8×10^{-6} unadjusted). The minor allele frequency of rs9939609 differs very little across our studies from Finland, Italy, and many different regions in the UK ranging from 0.38 to 0.40 in all except the second-smallest study, where it was 0.44. We found no significant regional variation in allele frequency in UK type 2 diabetic patients, whether testing 4 (P = 0.41) or 11 (P = 0.22) geographical regions of residence. For all these reasons, we do not believe that stratification/structure effects provide a realistic interpretation of our findings.

We have shown that common variation in the *FTO* gene is reproducibly associated with BMI and obesity from childhood into old age.

SNP rs9939609 lies within the first intron of the *FTO* gene and, based on information from HapMap, is highly correlated ($r^2 > 0.5$), with 45 additional SNPs within a 47-kb region that encompasses parts of the first two introns as well as exon 2 of *FTO*. There are no features to suggest that any of these SNPs represents the functional variant. Linkage disequilibrium between the BMI-associated SNPs and other variants falls rapidly outside the 47-kb region, such that there are no SNPs correlated at $r^2 > 0.2$ outside a 90-kb interval (Fig. 1 and fig. S2). Sequencing of 47 individuals selected for BMI > 40 kg/m^2 has revealed no clear candidate functional variants in the *FTO* coding region and minimal splice sites or 3′ UTR to explain the association (table S4). *FTO* is closely adjacent to a gene of unknown function *KIAA1005* (Fig. 1 and fig. S2), which is transcribed in the opposite direction. This opens up the possibility that genetic variation affects a regulatory element for *KIAA1005*; however, there is no obvious such variant within the 47-kb associated region. We conclude that the 47-kb intron within the *FTO* gene is most likely to contain the predisposing variant(s), but there is, at present, no clear genetic mechanism to explain how this alters the function or expression of *FTO, KIAA1005*, or more distant genes.

FTO is a gene of unknown function in an unknown pathway that was originally cloned as a result of the identification of a fused-toe (*Ft*) mutant mouse that results from a 1.6-Mb deletion of mouse chromosome 8 (*18*). Three genes of unknown function (*Fts, Ftm* and *Fto*), along with three members of the Iroquois gene family (*Irx3, Irx5*, and *Irx6* from the *IrxB* gene cluster), are deleted in *Ft* mice (*18*). The homozygous *Ft* mouse is embryonically lethal and shows abnormal development, including left/right asymmetry (*19*). Heterozygous animals survive and are characterized by fused toes on the forelimbs and thymic hyperplasia but have not been reported to have altered body weight or adiposity (*19*). The fused-toe mutant is a poor model for studying the role of altered *Fto* activity, because multiple genes are deleted. Neither isolated inactivation nor overexpression of *Fto* has been described.

We used reverse transcription PCR to assess the expression of *FTO* and *KIAA1005* in a human tissue panel (*18*). *FTO* was found to be widely expressed in fetal and adult tissues, with expression highest in the brain (fig. S3A). The transcription start site of *KIAA1005* lies only 200 base pairs from the 5′ end of *FTO* and ~61 kb from the 47-kb interval containing the BMI associations. *KIAA1005* is also ubiquitously expressed with relatively high levels in hypothalamus and islet (fig. S3B). The similarity of expression profile between these two transcripts may indicate joint transcriptional regulation but does not provide insights into which of the two genes is more likely to be involved. Further work with both knockout and overexpression

models of *FTO* and *KIAA1005* are likely to provide the most fruitful approach to understanding the mechanism and pathways whereby these variants influence the risk of obesity.

References and Notes

1. C. L. Ogden *et al.*, *JAMA* **295**, 1549 (2006).
2. H. H. M. Maes, M. C. Neale, L. J. Eaves, *Behav. Genet.* **27**, 325 (1997).
3. I. S. Farooqi, S. O'Rahilly, *Endocr. Rev.* 10.1210/er.2006-0040 (2006).
4. P. Boutin *et al.*, *PLoS Biol.* **1**, 361 (2003).
5. D. Meyre *et al.*, *Nat. Genet.* **37**, 863 (2005).
6. M. M. Swarbrick *et al.*, *PLoS Biol.* **3**, 1662 (2005).
7. C. J. Groves *et al.*, *Diabetes* **55**, 1884 (2006).
8. M. N. Weedon *et al.*, *Diabetes* **55**, 3175 (2006).
9. A. Herbert *et al.*, *Science* **312**, 279 (2006).
10. R. J. F. Loos, I. Barroso, S. O'Rahilly, N. J. Wareham, *Science* **315**, 179c (2007).
11. D. Rosskopf *et al.*, *Science* **315**, 179d (2007).
12. C. Dina *et al.*, *Science* **315**, 179b (2007).
13. Materials and methods are available as supporting material on *Science* Online.
14. J. P. Higgins, S. G. Thompson, J. J. Deeks, D. G. Altman, *BMJ* **327**, 557 (2003).
15. T. Lobstein, L. Baur, R. Uauy, *Obes. Rev.* **5**, 4 (2004).
16. S. Zhang, X. Zhu, H. Zhao, *Genet. Epidemiol.* **24**, 44 (2003).
17. A. L. Price *et al.*, *Nat. Genet.* **38**, 904 (2006).
18. T. Peters, K. Ausmeier, R. Dildrop, U. Rüther, *Mamm. Genome* **13**, 186 (2002).
19. F. van der Hoeven *et al.*, *Development* **120**, 2601 (1994).
20. Collection of the type 2 diabetes cases was supported by Diabetes UK, British Diabetic Association Research, and the UK Medical Research Council (Biomedical Collections Strategic Grant G0000649). The UK Type 2 Diabetes Genetics Consortium collection was supported by the Wellcome Trust (Biomedical Collections Grant GR072960). The ALSPAC study was supported by the UK Medical Research Council (MRC), the Wellcome Trust, and the University of Bristol. The British Women's Heart and Health Study was funded by the Department of Health and the British Heart Foundation. The Caerphilly study was funded by MRC and the British Heart Foundation. The Caerphilly study was undertaken by the former MRC Epidemiology Unit (South Wales) and was funded by the MRC. The data archive is maintained by the Department of Social Medicine, University of Bristol. The Exeter Family Study of Childhood Health was supported by NHS Research and Development and the Wellcome Trust. The work on the Northern Finland birth cohort study was supported by the Academy of Finland (104781), MRC (G0500539), and the Wellcome Trust (Project Grant GR069224). Oxford Biobank was supported by the British Heart Foundation. The Invecchiare in Chianti (InCHIANTI) study was supported by contract funding from the U.S. National Institute on Aging (NIA), and the research was supported in part by the Intramural Research Program, NIA, NIH. The European Prospective Investigation of Cancer (EPIC)–Norfolk cohort study is supported by program grants from MRC and Cancer Research UK. The EPIC-Norfolk obesity case-cohort study and its genotyping was funded by the Wellcome Trust and MRC. The genome-wide association genotyping was supported by the Wellcome Trust (076113), and replication genotyping was supported by the Wellcome Trust, Diabetes UK, the European Commission (EURODIA LSHG-CT-2004-518153), and the Peninsula Medical School. Personal funding comes from the Wellcome Trust (A.T.H., Research Leave Fellow; I.B., Investigator; E.Z., Research Career Development Fellow; L.R.C., Principal Research Fellow); MRC (J.R.B.P.); Diabetes UK (R.M.F.); and Throne-Holst Foundation (C.M.L.). L.W.H. is a Research Councils UK Diabetes and Metabolism Academic Fellow. M.N.W. is Vandervell Foundation Research Fellow at the Peninsula Medical School. C.N.A.P. and A.D.M. are supported by the Scottish executive as part of the Generation Scotland Initiative. We acknowledge the

Bat Flight Generates Complex Aerodynamic Tracks

A. Hedenström,[1]* L. C. Johansson,[1] M. Wolf,[1] R. von Busse,[2] Y. Winter,[2,3]† G. R. Spedding[4]

The flapping flight of animals generates an aerodynamic footprint as a time-varying vortex wake in which the rate of momentum change represents the aerodynamic force. We showed that the wakes of a small bat species differ from those of birds in some important respects. In our bats, each wing generated its own vortex loop. Also, at moderate and high flight speeds, the circulation on the outer (hand) wing and the arm wing differed in sign during the upstroke, resulting in negative lift on the hand wing and positive lift on the arm wing. Our interpretations of the unsteady aerodynamic performance and function of membranous-winged, flapping flight should change modeling strategies for the study of equivalent natural and engineered flying devices.

Bats and birds represent two independent evolutionary pathways solving the same problem: powered vertebrate flight. The smaller species show similar wing morphology, kinematics, and flight speeds and operate at similar Reynolds number (*1*). However, the wings of bats and birds also differ in some important respects. For example, the primary feathers of a bird wing can be separated so air can pass through as in a Venetian blind to produce a feathered (and aerodynamically inactive) upstroke. Although bat wing membranes can be actively stretched and collapsed (*2*), they probably cannot be made aerodynamically inactive as easily as bird wing feathers. Flapping wings generate trailing vortices containing information about the time-history and magnitude of the aerodynamic force produced during the wingbeat, and so wake vortices act as an aerodynamic footprint marking the previous passage of the animal through the air (*3–10*). The equivalence of forces exerted between a solid object and the surrounding fluid is a consequence of Newton's laws and has long been exploited to estimate drag forces from wake momentum fluxes (*11, 12*). Similarly, for a lifting body immersed in a uniform flow of speed U, the aerodynamic lift per unit of span can be written as $L' = \rho U \Gamma$, where ρ is air density and Γ is the circulation on the wing section. In the absence of

viscosity, vorticity and circulation are conserved according to Helmholtz's laws, and so any change in aerodynamic force (and hence circulation on the wing) must be associated with the shedding into the wake of vorticity of opposite sign, whose circulation matches the change on the wing.

The wake vortices of three bird species have recently been studied in some detail across wide speed ranges (*8, 10, 13*), whereas those of bats have received comparatively little attention (*6*). In the one qualitative study of airflows behind bats passing through a bubble cloud (*6*), the bats were reported to generate single vortex loops from each downstroke (with an inactive upstroke) at slow speed, whereas at a faster cruising speed, a pair of undulating vortices trailed the path of the wingtips throughout the wingbeat, implying that the upstroke generated lift. However, kinematic studies show a wingtip reversal during the upstroke during hovering and slow speed in bats (*14–19*), suggesting a reversal of the wing circulation during the upstroke, whose signature should be observable in the wake.

We made a systematic and quantitative study of the variation in wake topology and relative down- and upstroke function with flight speed in a small nectar-feeding phyllostomid bat species, *Glossophaga soricina*. Although detailed kinematics data are available for this species across a speed range from 1.2 to 7.5 m/s (*19*), it is impossible to infer the wake vortex distribution from kinematics alone (*19*). The aim was also to test the hypotheses, based on kinematics, that (i) the backward flick of the wing at slow speeds, as inferred on the basis of kinematics, generates lift and thrust (*14, 16, 17, 19*); and (ii) that the negative angle of attack during the upstroke at moderate speeds generates negative lift (*14, 16, 19*). Images of the wake were

analyzed by means of a digital particle image velocimetry (DPIV) method, and the quantitative measures of wake vorticity and total circulation were used to deduce the magnitude of aerodynamic forces and construct the wake topology (*20*).

We studied the wakes generated by two adult *G. soricina* individuals across the speed range from 1.5 to 7 m/s [body mass, 11 g; wingspan, 0.24 m; aspect ratio, 6.3 (*21*); Reynolds number (Re) $\approx 4 \times 10^3$ to 18×10^3; Strouhal number (St) ≈ 0.27 to 0.81 (*22*)]. Two orientations of the image plane were used: (i) a vertical streamwise plane aligned with the flow at three different positions along the wing span (outer wing, inner wing, and mid-body), and (ii) a cross-stream plane aligned perpendicular to the flow direction (Trefftz plane) (*20*).

We focus our presentation of the wakes on slow (1.5 m/s), medium (4 m/s), and high (6.5 m/s) speeds, which cover the natural range of forward speeds (*19, 23*). At slow speed (top row of Fig. 1), a strong start vortex, formed at the beginning of the downstroke, can be seen across the span (red blobs at right in Fig. 1, A to C, marked 1 in Fig. 1A). At the transition from downstroke to upstroke, the wing goes through a large supination (pitch-up rotation), so that the wing is flipped upside down. At this point, a combined stop-and-start vortex is shed (blue blob, left side of Fig. 1, A to C). During the upstroke, the wing moves backward faster than the forward speed, with circulation reversed, and the induced flow in the wake is primarily a backward-directed jet. Thus, the net aerodynamic force is forward (thrust) and upward (lift). At the following transition from upstroke to downstroke, the wings pronate rapidly (a pitch-down rotation), to shed a combined start/stop vortex for the next downstroke. This start/stop vortex (2 in Fig. 1A) appears above the previous one (1 in Fig. 1A) because the wake has convected downward in the interim. At the higher flight speed of 4 m/s, illustrated in the next two rows of Fig. 1 (panels D to F for downstroke and G to I for upstroke), the wake structure is quite different. The downstroke generates a strong start vortex (red patches in Fig. 1, D to F). The corresponding stop vortex is weaker and more diffuse, increasingly so as we move from outer wing (Fig. 1D) to inner wing (Fig. 1E) and body (Fig. 1F) image planes. Trace amounts of negative (blue) vorticity can be seen throughout the wingstroke. The associated induced velocity field (vectors in Fig. 1, D to F) shows a downward- and backward-directed momentum

[1]Department of Theoretical Ecology, Lund University, SE-223 62 Lund, Sweden. [2]Department of Biology, University of Munich, Germany. [3]Max-Planck Institute for Ornithology, Seewiesen, Germany. [4]Department of Aerospace and Mechanical Engineering, University of Southern California, Los Angeles, CA 90089–1191, USA.

*To whom correspondence should be addressed. E-mail: anders.hedenstrom@teorekol.lu.se
†Present address: Department of Biology, Bielefeld University, D-335 01 Bielefeld, Germany.